MAGNETOHYDRODYNAMICS Vol. 53 (2017), No. 3, pp. 483–494

TURBULENT MHD HEAT TRANSFER IN LIQUIDS WITH THE PRANDTL NUMBER Pr>1

A.V. Kotlyar[1], *T.E. Krasnoschekova*[1], *L.A. Sukomel*[1], *I.A. Belyaev*[2], *E.V. Sviridov*[1], *V.G. Sviridov*[2]

[1] *Moscow Power Engineering Institute (MPEI), Moscow, Russia*
[2] *Joint Institute of High Temperatures Russian Academy of Science (JIHT RAS), Moscow, Russia*

A simple mathematical model is proposed to analyze turbulent MHD flow and heat transfer for liquids with the Prandtl number Pr>1, exposed to a transverse magnetic field. Regime parameters corresponding to the operating conditions of thermo-nuclear sources of neutrons cooled by molten salts are considered. A numerical algorithm has been implemented for solving a system of conservation equations with account of the magnetic field influence on turbulent momentum and heat transfer. The algorithm has been verified against the experimental data on heat transfer and mean temperature profiles for a turbulent water flow in a circular tube without magnetic field action. Parametric calculations of the transverse magnetic field effect on the flow and heat transfer in a circular tube were made. The results are compared with the experimental data on the flow of 30% KOH aqueous solution as a model liquid.

Introduction. In recent years, interest in using molten salts as an alternative to liquid metal coolants in nuclear and fusion reactors has revived. Molten salts, such as lithium and beryllium fluorides ($LiFBeF_2$ or FLiBe) or alkali metal fluorides (LiFNaFKF or FLiNaK) are assumed as potential coolants and working fluids in the cooling systems of promising nuclear reactors and hybrid Tokamak reactors, which are sources of thermo-nuclear neutrons. Designing new, molten salt cooled power installations requires, in particular, reliable information about the action of magnetic fields, natural convection and temperature dependence of coolant properties on hydrodynamics and heat transfer. On the other hand, for liquids with Prandtl numbers exceeding unity, which molten salts belong to, these problems have hardly been studied at all, and the very limited available experimental information [1, 2] suggests that these effects might be significant even at relatively low Hartmann numbers and, therefore, must not be neglected.

To solve these problems and develop physical and numerical models of the above-mentioned processes, reliable experimental information about a spatial (or 3D) distribution of velocity or temperature in molten salt flows is badly needed. However, laboratory experiments with molten salts encounter great difficulties. The main problem here is the high melting point of FliBe or FLiNaK (about 450°C). Obviously, the working temperatures in the test loop should be well above that value, which restricts the use of most transducers and probe methods for local measurements of the velocity and temperature in the flow.

In fact, available experimental techniques make it possible to obtain the required data using only model liquids (with thermo-physical properties similar to those of molten salts) among which are, in particular, water or electrolyte aqueous solutions.

Thus, information about 3D distributions of the average and fluctuating characteristics of the temperature field in a fluid flow (i.e. local flow characteristics) is needed for valid physical or numerical modelling. Three-dimensionality provides information about the distribution of the local characteristics along the length of

the heated section and over the flow cross-section. No similar experiments with molten salt flows have been performed yet. This is quite reasonable because of significant engineering and methodical difficulties of such investigations. Moreover, considering the high temperatures and extreme corrosiveness of the working fluids, among which are molten salts, "precision" measurements by a microprobe introduced into the flow can hardly be made. Hence, simulation (either experimental with model liquids or numerical) is in fact the only method for investigating the heat transfer and hydrodynamics in molten salt flows.

At present, water or electrolyte aqueous solutions are used as model liquids in many studies. Note that electrolyte aqueous solutions are eminently suitable for studying heat transfer in liquids with Pr>1.

Another line of the investigation into the molten salt heat transfer is computer simulations based on the system of Reynolds-averaged Navier–Stokes equations (RANS) or on direct numerical simulations (DNS). The best approach to this problem is simultaneous performance of numerical calculations and physical experiments, with the results of the latter used to verify the developed computer codes. In this paper, the first version of the mathematical model and a numerical algorithm for investigating the turbulent MHD flow and heat transfer at low Ha and Re are presented. The model predictions have been verified against the experimental data for a water flow in a circular pipe. Parametric calculations were made to study the influence of the transverse magnetic field on the flow and heat transfer. The predictions are compared with the available experimental data for KOH aqueous solution flows.

1. Problem formulation. The magnetic field influence on hydrodynamics and heat transfer is intricate. In a turbulent flow, the influence of the magnetic field is generally twofold: it affects the averaged flow by deforming the velocity profile (Hartmann effect) and suppresses turbulent fluctuations. The extent to which the magnetic field affects the averaged flow depends on the mutual orientation of the magnetic field induction vector and averaged flow velocity vector and on the relation between Ha and Re, i.e. on the MHD interaction parameter $\mathrm{Ha}^2/\mathrm{Re}$.

The magnetic field interacts with the component of the averaged or fluctuating velocity vector orthogonal to the magnetic induction vector. In general, this initiates additional hydrodynamic and thermal effects to be described by additional terms in the conservation equations as applicable. Moreover, the system of conservation equations should be supplemented with the magnetic electrodynamics equations. However, in some cases, the interaction of the magnetic field with the averaged flow is either absent or negligible, hence, enabling the mathematical model formulation to be simplified considerably. Under these conditions, the magnetic field affects the fluctuating velocity component alone, with direct impact on the velocity fluctuation component orthogonal to the magnetic field induction vector, whereas the longitudinal component is affected indirectly via the energy exchange mechanism due to the pressure fluctuations. Then the system of conservation equations will have the same form as in the case without the magnetic field, and the magnetic field influence is accounted for by the terms describing the turbulent transport of momentum and heat. These regimes occur, first, in a longitudinal magnetic field and then in a transverse magnetic field at low values of $\mathrm{Ha}^2/\mathrm{Re}$, as demonstrated in Fig. 1*a* from [3], where the experimental friction factor ξ is presented as a function of Ha/Re for a flow in a circular pipe exposed to a transverse magnetic field. There is a third factor of the external magnetic field effect on the MHD flow in pipes associated with the relative electrical conductivity of the channel wall, in this study it is ignored.

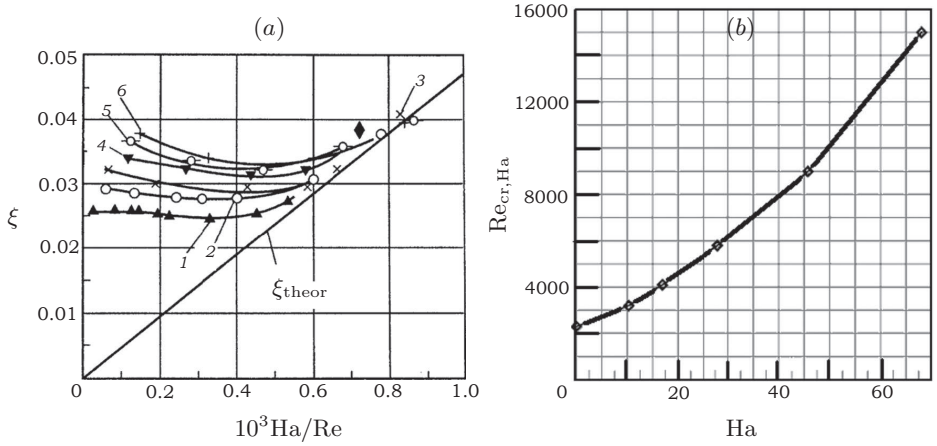

Fig. 1. Magnetic field effect on turbulent MHD flow in a circular pipe: (*a*) experimental friction factors [3], Re = 12000 (*1*), 7000 (*2*), 5000 (*3*), 3930 (*4*), 3325 (*5*), 2750 (*6*); (*b*) critical Reynolds number $\mathrm{Re}_{\mathrm{cr,Ha}}$ as a function of Ha.

It is evident from Fig. 1*a* that at low Reynolds numbers the magnetic field superimposed on the turbulent flow first decreases the friction factor and with the further increase of the Hartmann number the friction factor starts to grow approaching the asymptotic correlation $\xi = K \cdot (\mathrm{Ha}/\mathrm{Re})$ specific for a laminar flow at high Hartmann numbers. A similar behavior is also observed in channels with a different cross-section shape [3]. $K = 32$ for a plane channel and $K = 47$ for a circular pipe.

The decrease of the friction factor at low Reynolds numbers is caused by the suppression of the turbulent transport of momentum by the magnetic field, indicating that there are MHD flow regimes under the transverse magnetic field when the Hartmann effect is still of no importance.

The magnetic field suppresses the velocity fluctuations and prevents the appearance of new ones, i.e. the critical Reynolds number in the magnetic field $\mathrm{Re}_{\mathrm{cr,Ha}}$ increases with Ha. Fig. 1*b* displays $\mathrm{Re}_{\mathrm{cr,Ha}}$ vs Ha curve for a liquid metal flow in a circular pipe plotted considering the experimental data for the friction factor given in [4].

The estimations made by the designers of the Tokamak reactors cooled by molten salts demonstrate that the Hartmann numbers do not exceed $\mathrm{Ha} \leq 50$. The distinguishing feature of these MHD flows is that turbulence has already been suppressed in them, and the direct action of the magnetic field on the averaged velocity hardly manifests itself at all (i.e. the Hartmann effect is negligible). Therefore, at this stage of investigation, only the MHD flows, whose averaged characteristics are not affected by the magnetic field, will be analyzed. Then, as already noted above, the system of averaged conservation equations will have the form as in the case without the magnetic field action,

$$\frac{\partial \overline{U}_i}{\partial x_i} = 0, \tag{1}$$

$$\rho\left(\frac{\partial \overline{U}_i}{\partial t} + \overline{U}_k \frac{\partial \overline{U}_i}{\partial x_k}\right) = -\frac{\partial \overline{P}}{\partial x_i} + \frac{\partial}{\partial x_k}\left[\left(\eta \frac{\partial \overline{U}_i}{\partial x_k} - \rho\overline{u_i u_k}\right)\right], \tag{2}$$

$$\rho c\left(\frac{\partial \overline{T}}{\partial t} + \overline{U}_k \frac{\partial \overline{T}}{\partial x_k}\right) = \frac{\partial}{\partial x_k}\left[\lambda \frac{\partial \overline{T}}{\partial x_k} - \rho c\overline{u_k \vartheta}\right], \tag{3}$$

where t stands for the time; x_i, x_k are the spatial coordinates; $\overline{U}_i$, $\overline{U}_k$ are the averaged velocity vector components, $\overline{P}$ is the pressure, ρ is the liquid density, η is the liquid dynamic viscosity, λ is the liquid thermal conductivity, and c is the liquid heat capacity.

The terms $\rho\overline{u_i u_k}$ stand for additional stresses in the flow induced by the turbulent momentum transfer (i.e. the Reynolds stresses), and the terms $\rho c\overline{u_k \vartheta}$ describe the turbulent heat transfer. The specific form of these terms is determined by the peculiarities of the magnetic field influence on the turbulent transport. According to the Boussinesq hypothesis about the gradient behavior of turbulent transport, the momentum eddy diffusivity ε_σ and the heat eddy diffusivity ε_q are introduced as

$$-\rho\overline{u_i u_k} = \varepsilon_\sigma \frac{\partial \overline{U}_i}{\partial x_k}$$

and

$$-\rho c\overline{u_k \vartheta} = \varepsilon_q \frac{\partial \overline{T}}{\partial x_k}.$$

The heat eddy diffusivity ε_q is usually expressed via the eddy diffusivity for momentum as

$$\frac{\varepsilon_q}{a} = \frac{\nu}{a}\frac{\varepsilon_q}{\varepsilon_\sigma}\frac{\varepsilon_\sigma}{\nu} = \frac{\mathrm{Pr}}{\mathrm{Pr_T}}\frac{\varepsilon_\sigma}{\nu}.$$

The turbulent Prandtl number $\mathrm{Pr_T} = \varepsilon_\sigma \cdot \varepsilon_q$ is usually taken equal to unity. This assumption is confirmed in [5] by comparing the experimental distributions of the averaged temperature measured in a turbulent water flow with the available correlations for calculating the $\mathrm{Pr_T}$ distribution in the channel cross-section. The comparison demonstrates that using various theoretical correlations for $\mathrm{Pr_T}$ gives no advantage for the approach when $\mathrm{Pr_T}$ is assumed constant over the cross-section. The best agreement between the experimental data and the predictions was observed at $\mathrm{Pr_T} = 1 \div 0.9$.

As to the MHD flow, the eddy diffusivity $(\varepsilon_\sigma/\nu)_{\mathrm{Ha}}$ must consider the influence of the magnetic field on turbulence. The predictions presented below were obtained using the physical model proposed in [6, 7]. Various experimental data on the characteristics of the velocity and temperature fields in the turbulent MHD flow made it possible to conclude [6] that the magnetic field suppresses the turbulent transport in the channel cross-section more or less uniformly. Thus, the eddy diffusivity $(\varepsilon_\sigma/\nu)_{\mathrm{Ha}}$ can be presented as

$$\left(\frac{\varepsilon_\sigma}{\nu}\right)_{\mathrm{Ha}} = \gamma \left(\frac{\varepsilon_\sigma}{\nu}\right)_0, \tag{4}$$

where γ is the coefficient of the turbulent transport suppression by the magnetic field, which depends on the flow conditions, on the orientation of the magnetic field induction vector about the flow direction, on the channel cross-section shape and is independent of the transverse coordinate; $(\varepsilon\sigma/\nu)_0$ is the eddy diffusivity for the momentum with no magnetic field impact.

The validity of this approach has been confirmed for a flow in a circular pipe subjected to a longitudinal magnetic field [6] and for a plane channel flow in a transverse magnetic field [7].

The approach (4) is applied in this study to analyze the flow in a circular pipe under the action of a transverse magnetic field. The correlation proposed in [7] for the flow of conducting liquid in a plane channel exposed to a transverse magnetic field is used as the first approximation for γ.

The factor $\gamma(\mathrm{Re}, \mathrm{Ha})$ is described by an exponential function, the coefficients of which were found to fit the experimental data on velocity profiles and hydraulic resistance coefficients:

$$\gamma = \begin{cases} 1 - \exp\left[-k\left(\dfrac{\mathrm{Re} - \mathrm{Re}_{\mathrm{cr,Ha}}}{\mathrm{Re}_{\mathrm{cr,Ha}}}\right)^{0.8}\right] & \text{for } \mathrm{Re} \geq \mathrm{Re}_{\mathrm{cr,Ha}}, \\ 0 & \text{for } \mathrm{Re} < \mathrm{Re}_{\mathrm{cr,Ha}}, \end{cases} \tag{5}$$

where $k = 3.75/\mathrm{Ha}^{0.7}$ for $3 \leq \mathrm{Ha} \leq 20$ and $k = 0.46$ for $20 \leq \mathrm{Ha} \leq 100$.

The influence of the channel cross-section shape on the coefficient γ is considered using the critical Reynolds number $\mathrm{Re}_{\mathrm{cr,Ha}}$, which was determined from the available experimental data (see Fig. 1*b*).

2. Verification of the mathematical model. The above mathematical model has been verified against the experimental data on integral and local characteristics of the temperature field in turbulent liquid flows. The verification process included two stages. The numerical algorithm was validated first by comparing the predictions with the experimental data on heat transfer and temperature distributions for a turbulent non-isothermal water flow in a circular pipe without the magnetic field action [5]. At the second stage, parametric calculations of an MHD flow of conducting liquid with Pr>1 in a transverse magnetic field in a circular pipe were made. The predictions were compared with the experimental data from [1, 2] for a flow of 30% aqueous KOH solution.

The investigated cases [1, 2, 5] refer to a steady-state flow with axisymmetric velocity and temperature fields. According to the experimental conditions [1, 2, 5], the temperature dependence of liquid properties can be neglected. Hence, the system of conservation equations (1)–(3) can be written as

$$\frac{1}{r}\frac{\partial}{\partial r}\left(r\overline{U}_r\right) + \frac{\partial \overline{U}_x}{\partial z} = 0, \tag{6}$$

$$\rho\left(\overline{U}_x\frac{\partial \overline{U}_x}{\partial x} + \overline{U}_r\frac{\partial \overline{U}_x}{\partial r}\right) = -\frac{\partial \overline{p}}{\partial x} + \frac{1}{r}\frac{\partial}{\partial r}\left[r\left(\eta + \varepsilon_\sigma\right)\frac{\partial \overline{U}_x}{\partial r}\right], \tag{7}$$

$$\rho\left(\overline{U}_r\frac{\partial \overline{U}_r}{\partial x} + \overline{U}_r\frac{\partial \overline{U}_r}{\partial r}\right) = -\frac{\partial \overline{p}}{\partial x} + \frac{1}{r}\frac{\partial}{\partial r}\left[r\left(\eta + \varepsilon_\sigma\right)\frac{\partial \overline{U}_r}{\partial r}\right], \tag{8}$$

$$\rho c\left(\overline{U}_x\frac{\partial \overline{T}}{\partial x} + \overline{U}_r\frac{\partial \overline{T}}{\partial r}\right) = -\frac{\partial \overline{p}}{\partial x} + \frac{1}{r}\frac{\partial}{\partial r}\left[r\left(\lambda + \varepsilon_q\right)\frac{\partial \overline{T}}{\partial r}\right], \tag{9}$$

In the calculations, $(\varepsilon_\sigma/\nu)_0$ was determined using the correlations proposed in [8] for a relatively low $\mathrm{Re} = (3 \div 20)\cdot 10^3$:

$$\frac{\varepsilon_\sigma}{\nu} = \begin{cases} 0.41\left[y^+ - y_B^+ \mathrm{th}\left(\dfrac{y^+}{y_B^+}\right)\right] & \text{for } 0 < y^+ < y_\delta^+, \\ \dfrac{0.41}{3}\left(y^+ - y_{B_1}^+\right)\left(R^2 + 0.5\right)(1 + R) & \text{for } y_\delta^+ < y^+ < y_0^+, \end{cases} \tag{10}$$

where

$$y_B^+ = 11.1 + \left(\frac{396}{y_0^+ + 100}\right)^{3.3} \tag{11}$$

$$y_\delta^+ = 9.2\left[\lg\left(y_0^+/237\right)\mathrm{th}\left(\frac{\lg\left(y_0^+/237\right)}{0.17}\right)\right] + 18.7, \tag{12}$$

$y_{B_1}^+$ was found provided Eq. (11) is equal to Eq. (12) at $y^+ = y_\delta^+$, $y_0^+ = r_0 u_*/\nu$.

With Re > 20000, the correlations (10) approach and then coincide with the known Reihardt expressions, which are still considered among the best semi-empirical correlations for the eddy diffusivity of momentum in circular pipes.

The system of equations (6)–(9) along with Eqs. (4), (5), (10) was solved numerically in a pipe of finite length having a heated section. A uniform velocity distribution was set at the inlet. A constant heat flux on the inside of the heated section was specified in accordance with the experimental conditions [1, 2, 5]. It was assumed in the calculations that at the inlet into the magnetic field the turbulence was immediately suppressed to a level characteristic of the specified Re and Ha.

The numerical algorithm was implemented in the ANES software package [9].

3. Verification of mathematical models against data for a flow not exposed to magnetic field. Without the magnetic field action, the predictions were compared with the experimental data obtained in [5] for a turbulent water flow. These experiments were performed in a $\varnothing 30 \times 0.45$ mm stainless steel smooth pipe. Before the heated section of $40d$ in length, there was a hydrodynamic entrance section of $70d$ in length. The experiments were performed in a range of Re = 4500–30000, with Pr = 5.2–8.6. The wall heat flux ranged from 9300 to 22000 $\mathrm{W/m^2}$. Under these experimental conditions, the effect of natural convention on heat transfer was almost completely eliminated. The difference between the wall temperature t_w and the pipe axis temperature was within 5–10°C and, therefore, the temperature dependence of water properties can be ignored.

Two differences between the results used for verification and the experimental data obtained in other investigations should be noted. First, the measurements were made [5] by a probe at many points, spaced by small intervals along the entire length of the heated pipe. Second, at each section, measurements were made at small steps along the radius, starting from the pipe axis and until the micro thermocouple contacted the wall. During the process, thorough measurements were made in the viscous sublayer (at about ten points across the sublayer thickness) that is especially important for the liquids with Pr>1.

The local measurements of heat transfer [5] demonstrate the behavior of the Nusselt number (Nu) along the heated section in detail. For Re = 4500–30000, a correlation of $\mathrm{Nu/Nu_\infty}$ in terms of the Reynolds number Re and longitudinal coordinate x/d is obtained as follows [5]:

$$\frac{\mathrm{Nu}}{\mathrm{Nu}_\infty} = 1 + \frac{22}{\mathrm{Re}^{0.49}} \exp\left[\frac{76}{\mathrm{Re}^{0.67}(x/d)} - 0.0017\mathrm{Re}^{0.63}(x/d)\right], \qquad (13)$$

with an error of ±4%. Therefore, the experiments [5] may be adopted as the "initial" state of the flow and heat transfer, with reference to which the effect of an additional complicating factor will be studied. It is evident that the first stage of the assessment of the mathematical model must be its verification against reliable experimental data for the above-mentioned initial state.

Fig. 2 shows the experimental and predicted temperature profiles for two Reynolds numbers in the developed heat transfer zone. The temperature profiles are presented in the dimensionless form $T^+ = f(y^+)$, where $T^+ = [t_\mathrm{w} - t(y)]/t_*$, $y^+ = yu_*/\nu$, $t_* = q_\mathrm{w}/(\rho c u_*)$, $u_* = \sqrt{\tau_\mathrm{w}/\rho}$, t_w is the wall temperature, t is the local flow temperature, y is the distance from the wall, q_w is the wall heat flux; τ_w is the wall shear stress, u_* is the dynamic velocity, ν is the kinematic viscosity. It is evident from Fig. 2 that the predictions are in excellent agreement with the experiment.

In the thermal inlet zone, the predictions by Eqs. (6)–(9), (10) also agree well with the experiment, as illustrated by Fig. 3. Typical predicted and measured

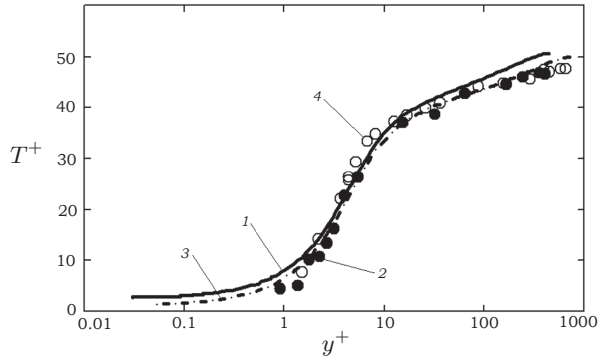

Fig. 2. Experimental and predicted distributions of the averaged velocity far away from the heated section inlet ($x/d = 34.43$); *1*, *3* – prediction by Eqs. (6)–(9), (10), *2*, *4* – experiment [5]; *1*, *2* – Re = 15000; *3*, *4* – Re = 27000.

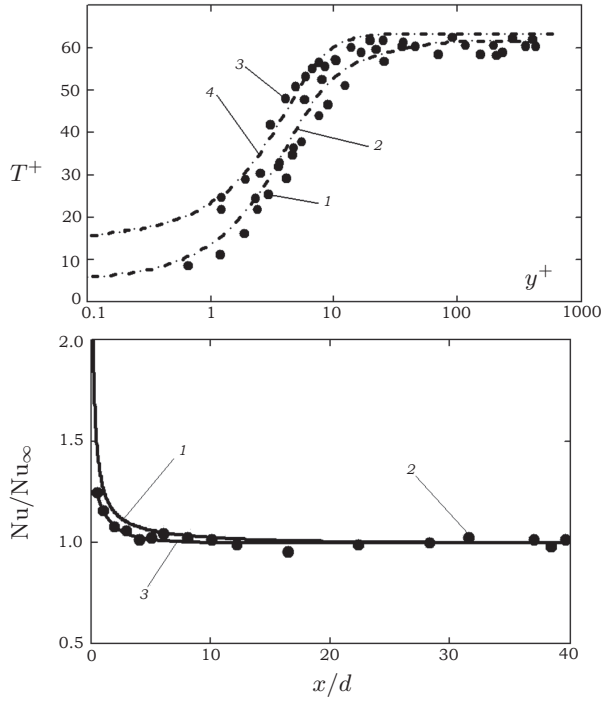

Fig. 3. Experimental and predicted temperature profiles within the thermal inlet zone (*a*) and the local heat transfer distribution along the heated section (*b*) for Pr = 7; (*a*) *1*, *3* – experiment [5], *1* – Re = 20500, $x/d = 12.15$; *3* – Re = 10000, $x/d = 4$; *2*, *4* – predictions by Eqs. (6)–(9) and (10), *2* – Re = 20500, $x/d = 12.15$; *4* – Re = 10000, $x/d = 4$; (*b*) Re = 11000, *1* – predictions by Eqs. (6)–(9), (10), *2* – experiment [5], *3* – interpolation correlation (13).

temperature profiles at various distances from the inlet of the heated section are presented in Fig. 3*a*. Excellent agreement is evident. Note that the good agreement between the predicted and the measured curves in Fig. 3*a* implicitly confirms the fact that the distributions of the longitudinal component of the averaged velocity vector hardly experienced any transformation within the heated section during the experiments [5].

The numerical modelling yielded a correlation of $\mathrm{Nu/Nu_\infty} = f(x/d)$ which reproduced the experimental data not only qualitatively but also quantitatively

(Fig. 3*b*). For all the regimes, the results of the calculation by ions using the mathematical model (6)–(9), (10) agree well with the predictions by the interpolation correlation (13).

The results presented above demonstrate that the mathematical model (6)–(9), (10) properly describes the considered real flow conditions and heat transfer and that the proposed numerical algorithm gives reasonable predictions. Therefore, the following estimations of the magnetic field influence on heat transfer can be considered substantiated.

4. Predictions of MHD heat transfer. As it was already mentioned above, this work included also an investigation of the influence of a transverse magnetic field on the heat transfer in a circular pipe at relatively low values of Ha/Re, when the Hartmann effect can be ignored. The results of the parametric calculations, using Eqs. (6)–(9) with Eqs. (4), (5) and (10), made it possible to estimate the influence of the magnetic field on the averaged temperature profiles and heat transfer. The predicted averaged temperature profiles and the Nusselt number Nu for a liquid MHD flow with Pr = 7 at Ha = 40 are compared in Fig. 4 with the corresponding characteristics for a flow not exposed to the magnetic field (Ha = 0) under the same flow conditions. It is evident from Fig. 4*a* that even at a relatively low Ha the external magnetic field deforms the temperature profiles significantly. In particular, at Re = 10000, the liquid temperature at the pipe axis increases by a factor of 4, if compared with a flow without the magnetic field influence, and at Re = 15000, a seven-fold increase of the temperature in this flow zone should be expected. Changes in distribution of the averaged flow temperature also affect the heat transfer coefficients. Fig. 4*b* illustrates the predicted distributions of the local Nu along the heated section at Re = 20000 and Pr = 7 for Ha = 0 and Ha = 40. In spite of the fact that at Ha = 40 complete laminarization of the flow, at least at a distance of $40x/d$ from the inlet into the heated section, is not predicted, a four-fold increase in heat transfer in the sufficiently long heated section can be expected, i.e. the effect of flow laminarization is quite substantial and should not be ignored in practice.

In addition to the parametric calculations, the mathematical model (6)–(9) with Eqs. (4), (5), (10) was tested against the experimental data from [1, 2]. These data were obtained when investigating an MHD flow of KOH aqueous solution (30%wt. KOH) in a horizontal circular pipe exposed to a transverse magnetic field.

These experiments involved the measurement of the local heat transfer coefficients along the length of the heated section and of the local flow temperatures. Using a comb-type micro thermocouple probe installed at a pipe section far away from the heated section inlet, the average temperature profiles and temperature fluctuation intensity profiles were measured at Ha = 0, 5, 10, 15. The experiments were performed to study the heat transfer of a working liquid flow in 8-m long pipes with a diameter of 50 or 89 mm in the range Re = 7400 – 46000 and with Pr = 4.85 – 9.8. The test sections included an upward not heated section of 3 m in length and a heated section 2.4 m long. The magnetic field was produced by a 1.4 m long solenoid, the inlet section of which was at a distance of 1.62 m from the inlet of the heated section. In the experiments, in a 50-mm diameter pipe (Re = 7400 – 20000, Pr = 4.85 – 5.23) the rack micro thermocouples could be traversed at a step of 0.02 mm using a micrometer feeding mechanism. The minimum distance, at which the thermocouple junction could approach the wall, was 0.05 mm. As a result, several experimental points were measured within the viscous sublayer [1, 2]. During the experiments [1, 2], it was attempted to maintain the experimental

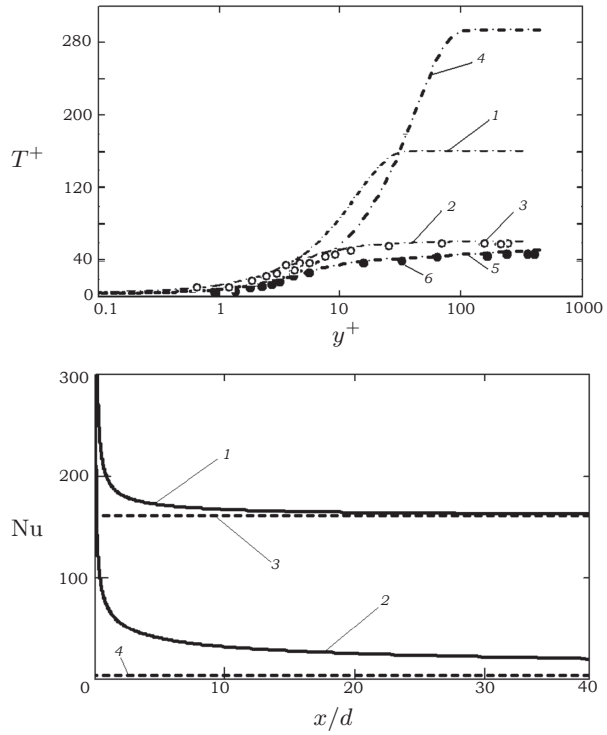

Fig. 4. Effect of a transverse magnetic field on average temperature profiles (a) and heat transfer (b) at Pr = 7; (a) *1*, *2*, *3* – Re = 10000, x/d = 4, *1* – predictions at Ha = 40, *2* – predictions at Ha = 0, *3* – experiment [5] at Ha = 0; *4*, *5*, *6* – Re = 15000, x/d = 34.43, *4* – predictions at Ha = 40, *5* – predictions at Ha = 0, *6* – experiment [5] at Ha = 0; (b) predictions at Re = 20000; *1* – Ha = 40, *2* – Ha = 0, *3* – Nu_∞ for turbulent flow, *4* – Nu_∞ for laminar flow.

conditions in order to minimize the effect of natural convection on the velocity and temperature fields, although at the low Re this effect could be hardly avoided. However, on the whole, the experiments [1, 2] correspond to the case examined in [5], i.e. to the development of the temperature field against the background of the almost completely developed velocity field.

The predictions are compared with the experiment in Figs. 5–7 (the presented results have to be processed using the procedure addressed in [1, 2]).

According to the data from [1, 2], at Ha = 20, the average temperature profiles presented as $T^+ = f(y^+)$ elongate in the flow core by 45% at Re = $9000 \div 11000$ or by 30% at Re = 20000. Unfortunately, the Prandtl number for these curves is not specified in [1, 2], making, for this reason, more difficult a comparison of the expermental data with the predictions. The predicted and the measured temperature profiles with Re = 5000, Pr = 6.2 and with four values of Ha = 0, 5, 10, 15 are compared in Fig. 5. The temperature curves are presented as $(T_\mathrm{w} - T)/(T_\mathrm{w} - T_0) = f(y/R)$, where T_w is the wall temperature, T is the current temperature, T_0 is the pipe axis temperature; y is the distance from the wall, R is the pipe radius. Inspite of the poor presentation of the temperature distribution, it is seen that with increasing Ha, the temperature gradient near the wall decreases, indicating the elongation of the temperature profile in the pipe core (the predicted curves in Fig. 5a). The corresponding exerimental profiles [1] are illustrated in Fig. 5b.

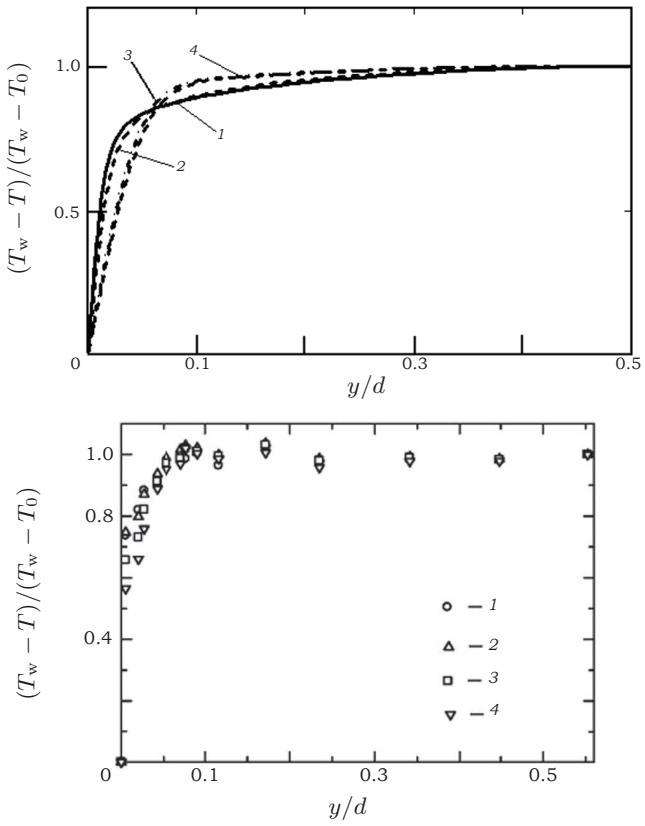

Fig. 5. Temperature profiles at Re = 5000, Pr = 6.2; *1* – Ha = 0, *2* – Ha = 5, *3* – Ha = 10, *4* – Ha = 15; (*a*) – predictions; (*b*) – experiment [1].

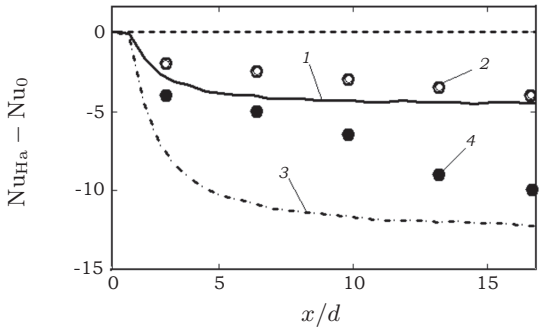

Fig. 6. Heat transfer in a transverse magnetic field as a function of the length for Re = 20000: predictions for Re = 20000: *1*, *2* – Ha = 10; *3*, *4* – Ha = 15; *1*, *3* – predictions by Eqs. (6)–(9) with Eqs. (4), (5), (10); *2*, *4* – experiments [1, 2].

The experimental and the predicted data on heat transfer are compared in Figs. 6 and 7. Fig. 6 shows the distribution of Nu along the length of the heated section for Re = 20000 and Ha = 0, 10, 15 as the correlation $\mathrm{Nu_{Ha}} - \mathrm{Nu_0} = f(x/d)$. Both the predicted and the experiental data demostrate a decrease in heat transfer along the heated section in the transverese magnetic field.

In this case, within $5 - 10x/d$ from the magnetic field inlet section, the calculations yield a more sharp decrease in heat transfer along the length, if compared

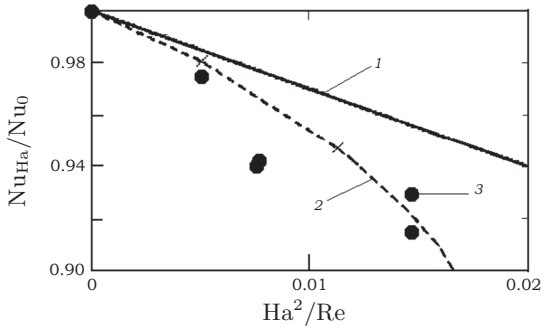

Fig. 7. Heat transfer far away from the inlet into the transverse magnetic field: *1* – experiment [10] in a square channel with 15% KOH solution, *2* – predictions by Eqs. (6)–(9) with Eqs. (4), (5), (10), *3* – experiments [1, 2].

with the experiments. This difference can be explained by an model assumption that at the inlet into the magnetic field the turbulent fluctuations are suppressed instantly to a level corresponding to a specified Hartmann number. It is seen in Fig. 6 that at a large distance from the magnetic field inlet the deviation of the predicted Nusselt numbers from the experimental values decreases.

The relative variation of Nu_{Ha} in the magnetic field as a function of Ha^2/Re far away from the magnetic field inlet is illustrated in Fig. 7. This figure is a fragment of the plot from [2], which illustrates the experimental Nu for KOH aqueous solutions in a transverse magnetic field for the Ha^2/Re range, where the assumption that the Hartmann number has a negligible impact on hydrodynamics and heat transfer is valid. In Fig. 7, the points represent the experimental data from [1, 2], the solid line (curve *1*) presents the experimental data [10] for the 15% KOH solution flow in a square channel with non-conducting walls. The dashed line (curve *2*) illustrates our numerical predictions for the 30% KOH solution flow in a circular pipe. It is appreciated from Fig. 7 that the predictions by Eqs. (6)–(9) with Eqs. (4), (5) and (10) for the circular pipe agree well with the experiment although it should be pointed out that in the examined Ha^2/Re range the experimental Nusselt numbers for a circular pipe and a square channel differ only slightly, with a maximum data disagreement of 5% (at $Ha^2/Re = 0.017$).

5. Conclusion.

1. A simple mathematical model is proposed to analyze the turbulent flow and heat transfer of liquids with Prandtl numbers Pr>1 in a transverse magnetic field, as applied to the operating conditions of thermo-nuclear neutron sources cooled by molten salts. The verification of the model and numerical algorithm against the experimental data for a water flow (without the magnetic field) demonstrated their usefulness and allowed a conclusion that further estimations of the magnetic field impact on heat transfer would be feasible.

2. The parametric calculations for a flow exposed to a magnetic field have revealed that the transverse magnetic field considerably affects the turbulent transport in molten salt flows, and this effect must not be ignored in practice. This finding was substantiated by verifying the mathematical model (6)–(9) with Eqs. (4), (5), (10) against the experimental results for the flow of a model conducting liquid. The predictions and the experiment agree well.

3. The further investigation are planned to be performed as follows: extension of the physical model of turbulent transport to a flow, the hydrodynamics and heat transfer of which are under the combined action of several factors, such as magnetic

field, natural convection and variation of liquid properties. In addition, the effect of the relative conductivity of the channel wall for the examined MHD flow should be studied.

Acknowledgments. The work is supported by RSCF project no. 1450-00124. The calculations are carried out in the Joint Supercomputer Center of the Russian Academy of Sciences.

References

[1] H. Nakaharai, J. Takeuchi, T. Yokomine *et al.* The influence of a magnetic field on turbulent heat transfer of a high Prandtl number fluid. *Experimental Thermal and Fluid Science*, vol. 32 (2007), pp. 23–28.

[2] T. Yokomine, J. Takeuchi, H. Nakaharai *et al.* Experimental investigation of turbulent heat transfer of high Prandtl number fluid flow under strong magnetic field. *Fusion Science and Technology*, vol. 52 (2007), no. 3, pp. 625–629.

[3] L.G. Genin, V.G. Sviridov. *Hydrodynamics and Heat Transfer in MHD Flows in Ducts* (Moscow, MPEI Publishing House, 2001.), 200 p. (in Russian).

[4] V.M. Borishansky, S.S. Kutateladze, I.I. Novikov, O.S. Fedinsky. *Liquid Metal Heat Transfer Media* (Moscow, Atomizdat, 1976, 3rd ed.), 328 p. (in Russian).

[5] I.A. Belyaev, O.D. Zakharova, T.E. Krasnoshchekova, V.G. Sviridov, L.A. Sukomel. The laboratory and numerical simulation of molten salts heat transfer in thermonuclear source of neutrons. Part 1. Heat transfer. *Heat Power Engineering*, vol. 63 (2016) no. 2, pp. 81–88.

[6] L.G. Genin, T.E. Krasnoschekova, V.G. Sviridov. Heat transfer of liquid metals flow in thermonuclear reactor of tokamak type. Problems in Nuclear Science and Technology. *Thermonuclear Synthesis*, no. 3 (1985), pp. 41–46 (in Russian).

[7] L.G. Genin, T.E. Krasnoschekova, E.V. Sviridov. Hydrodynamics and heat transfer of electric conducting fluid flow between parallel plates under a transverse magnetic field. *Thermophysics of High Temperatures*, vol. 36 (1998), no. 3, pp. 461–469.

[8] V.N. Popov, V.M. Belyaev. Heat transfer in transitional and turbulent flows in a circular tube at small Reynolds numbers. *Thermophysics of High Temperatures*, vol. 13 (1975), no 2, pp. 370–378 (in Russian).

[9] V.I. Artemov, G.G. Yankov. Numerical analysis of working efficiency of sectional air-conditioner with air heat exchanger. *Bulletin of Moscow Engineering Institute*, no. 6 (2010), pp. 155–160.

[10] A.Ya. Blum. The influence of magnetic field on heat transfer in turbulent flow of electrical conducting liquid. *Thermophysics of High Temperatures*, vol. 5 (1967), no. 1, pp. 79–86 (in Russian).

Received 22.05.2017